16th World Conference on Earthquake, 16WCEE 2017
Santiago Chile, January 9th to 13th 2017
Paper N° 664
Registration Code: S-L1460952409

# SEISMIC BEHAVIOR AND ASSESSMENT OF DRIFT-HARDENING CONCRETE COLUMNS

G. Sargsyan [1], G. Cai [2], T. Takeuchi [3], Y. Sun [4]

[1] Graduate school of engineering, Kobe University, Japan, sargsyangrigor@hotmail.com
[2] Faculty of engineering technology, Hasselt University, Kingdom of Belgium, gaochuang.cai@uhasselt.be
[3] Graduate school of engineering, Kobe University, Japan takeuchi_t@person.kobe-u.ac.jp
[4] Graduate school of engineering, Kobe University, Japan sun@person.kobe-u.ac.jp
…

## *Abstract*

This paper presents results of an experimental program undertaken to evaluate the seismic performance of concrete circular columns reinforced with ultra-high-strength (UHS) rebars for the purpose of development of resilient concrete columns which are expected to exhibit positive secondary stiffness till large drift and leave small and easily repairable residual deformation even after experiencing potential mega earthquakes. The use of UHS and low-bond strength rebars as longitudinal reinforcement of concrete columns offers several advantages over conventional ductile columns in maintaining stiffness and reducing residual deformation due to the long elastic region of the UHS rebars.
Specimens consisted of four 1/3 scale cantilever concrete columns reinforced by eight UHS and low-bond strength rebars (SBPDN 1275/1420) with spiraled groove on their surface. The columns had a circular section of 250 mm in diameter. The experimental variables were; the shear span ratio of column and the applied axial load level. The columns were transversely confined by thin steel plates. The steel plates were formed by connecting two pieces of pre-manufactured semi-circular plates through nuts and bolts.

*Keywords: Drift hardening; circular concrete column; residual deformation*

## 1. Introduction

Great Hanshin and Tohoku earthquakes, which struck Japan on January 17 of 1995 and March 11 of 2011 respectively had caused severe damage to many reinforced concrete (RC) buildings and infrastructures. Even the modern designed RC structures satisfying the seismic design provision were also observed to have moderate-to-major damages after those mega earthquakes.

Demolition and replacement of the moderate-to-major damaged RC building and structures have been a standard practice during restoration of an earthquake-damaged region in the world. However, this kind of practice often costs a lot and governments need to spend huge sources for it. That is why human society has recently required that the buildings and infrastructures must be safe not only during an earthquake but also after. Ensuring the usability and reparability of new and existing structures after great earthquakes represents one of the main issues in modern seismic engineering.

Nowadays the earthquake-resisting building members must have stable response of lateral-resistance without deterioration until large displacement even under high axial load, and small residual deformation after laterally deformed largely by mega earthquakes. One of the method to solve the above-mentioned problems is the use of high strength materials for creating a new type of hybrid concrete structures, which will consist of a resilient concrete frame and sets of energy absorption devices. Apparently, performance of this type of hybrid concrete structure is greatly dependent upon resilience and strength of the concrete frame. In order to improve the strength and resilience of concrete columns, the authors have suggested a combination of external confinement system employing thin steel plates and internal longitudinal reinforcement with UHS rebars in cocnrete columns.

Objective of this paper is to present an experimental and analytical study of the effectiveness of this method when applied to circular concrete columns that were laterally confined by bolted thin steel plates and longitudinally reinforced with SBPDN 1275/1420 rebars. To achieve these goals, four specimens were fabricated and tested under reversed cyclical lateral loading and constant axial compression. Parellel to the experimental work, an analytical method, which can take into account effect of the slippage of SBPDN rebar and confinement by bolted steel plates on seismic performacne of test specimens, was also presented. Validity and accuracy of the proposed method will be verified through comparing the theoretical results with the measured ones.

## 2. Outlines of the experiments and test apparatuses

### 2.1 Details of specimens

Fig. 1 shows the dimensions and reinforcement details of the four one-third scale cantilever columns, while Table 1 lists the primary experemental parameters along with the main test resuts. The mechanical properties of the used steels are summarized in Table 2.

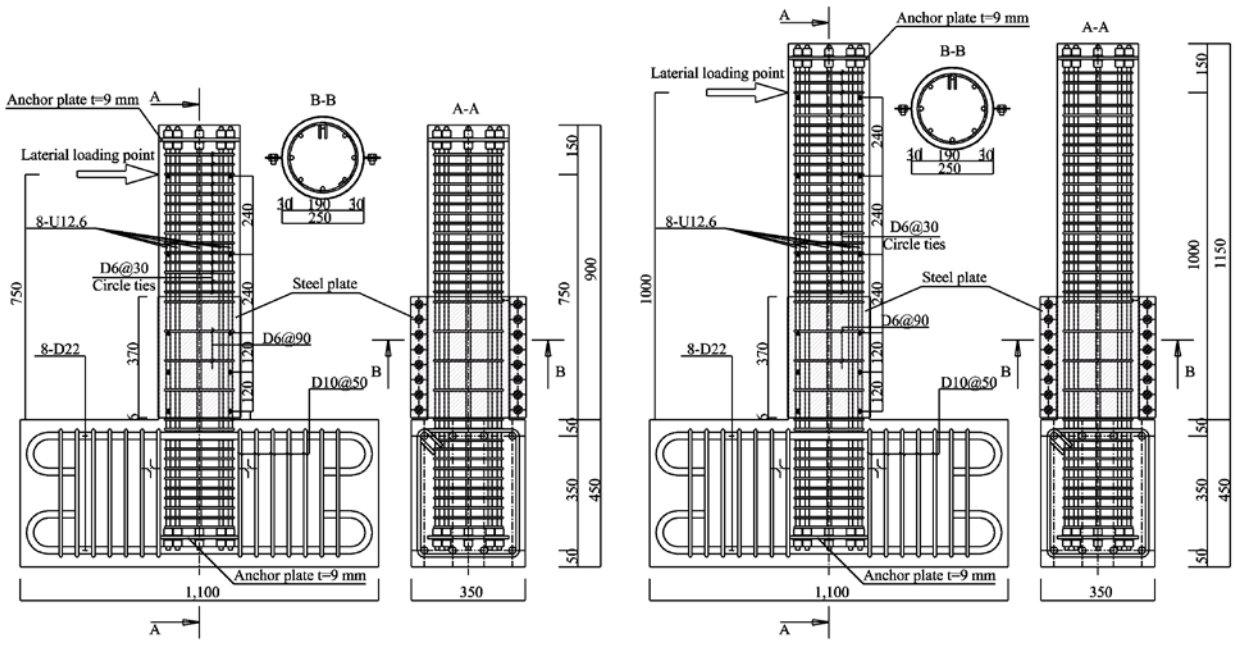


Fig. 1 Dimensions and reinforcement details of test columns

All columns had a round cross section of 250 mm in diameter and two different shear span ratios, 3.0 and 4.0, respectively. Ready mixed concrete made of Portland cement and coarse aggregates with maximum diameter of 20 mm was used to fabricate the specimens. İn each column, eight UHS (SBPDN1275/1420) rebars of 12.6 mm in diameter with specific yield strength of over 1275 N/mm$^2$ (see Table 2) and spiral groove (see Fig. 2) were distributed uniformly along the perimeter of column section. The bond-strength of UHS rebars are 3 N/mm$^2$ which is about one-fifth of that of ordinary deformed rebars when the rebar is embedded in the concrete with specified compressive strength of 40 N/mm$^2$ [1]. The longitudinal reinforcement ratio for the columns were 2.03%. As one can see from Fig. 1, each specimen was covered with steel plates of 1.6 mm in thickness and 370 mm (1.5D) in height from the column base, in addition to that the column was laterally confined by circular D6 hoop with 90mm and 30mm spacing for the steel plate confined region and the left, respectively. The steel plates were formed by connecting two pieces of pre-manufactured semi-circular plates through high strength bolts and nuts. In order for the steel plates not to directly sustain the axial stresses caused by external moment and axial load, clearance of 6 mm was provided between the steel plates and the column base.

Fig. 2 Surface shape of ultra-high strength (UHS) rebars

Table 1 Primary experemental parameters and main test resuts.

| Specimen | a/D | $f_c'$ (N/mm$^2$) | P (kN) | n | Longitudinal rebars | | Transverse reinforcement | | | $Q_{exp}$ (kN) | $R_{exp}$ (%) |
|---|---|---|---|---|---|---|---|---|---|---|---|
| | | | | | Type | $\rho_g$ (%) | t (mm) | $\rho_t$ (%) | $\rho_h$ (%) | | |
| RS30N33T | 3 | 43.2 | 699.0 | 0.33 | 8-U12.6 | 2.03 | 1.6 | 2.56 | 0.67 | 134.0 | 5.0 |
| RS30N45T | 3 | 43.1 | 953.0 | 0.45 | 8-U12.6 | 2.03 | 1.6 | 2.56 | 0.67 | 131.0 | 5.0 |
| RS40N33T | 4 | 43.3 | 701.0 | 0.33 | 8-U12.6 | 2.03 | 1.6 | 2.56 | 0.67 | 83.0* | 3.75* |
| RS40N10T | 4 | 42.4 | 208.0 | 0.10 | 8-U12.6 | 2.03 | 1.6 | 2.56 | 0.67 | 86.0 | 5.0 |
| Note: a/D -shear span ratio; $f_c'$ -concrete cylinder strength; P -axial force; n -axial load ratio; $\rho_g$ -the steel ratio of longitudinal rebar; t -thickness of steel plate; $\rho_h$ -the volumetric ratio of hoops; $\rho_t$ -the volumetric ratio of steel plate; $Q_{exp}$ -ultimate lateral load; $R_{exp}$ -drift angle at $Q_{exp}$.; *Loading was prematurely terminated in specimen RS40N33T when drift angle reached 0.04 rad due to disorder of measurement. | | | | | | | | | | | |

To measure strains in longitudinal rebars, strain guages were embedded via an adhesive to the surface of rebars located 25mm, 145mm, 265mm, 505mm and 745mm away from the end at the tensile and compressive sides of each column. A total of 16 strains gages were also used to measure the strains in steel plates and hoops.

Experimental variables were the shear span ratio (a/D) and axial load ratio (n). Specimens with shear span ratio of 3.0 were tested under axial load ratios of 0.33 and 0.45, while specimens with shear span ratio of 4.0 were tested under axial load ratios of 0.10 and 0.33 respectively.

Table 2 Mechanical properties of the steels

| Name | Type | $f_y$ (N/mm$^2$) | $\varepsilon_y$ (%) | $f_u$ (N/mm$^2$) | $E_s$ (kN/mm$^2$) |
|---|---|---|---|---|---|
| U12.6* | SBPDN 1275/1420 | 1377 | 0.84 | 1463 | 215 |
| D6 | SD295A | 394 | 0.21 | 522 | 197 |
| PL1.6* | SS400 | 273 | 0.32 | 405 | 201 |
| Note: $f_y$ -yield stress; $f_u$ -ultimate stress; $E_s$-Young's modulus; $\varepsilon_y$ -yield strain; $\varepsilon$* 0.2% offset yield strength. | | | | | |

## 2.2 Test setup and loading program

The tests were conducted using the setup shown in Fig. 3. The loading apparatus was designed to subject the column to reversed cyclic lateral load and constant axial compression. Vertical hydraulic jack with capacity of 1000 kN and connected to stiff loading via a roller was used to apply constant axial compression load, and the reversed cyclic lateral load was applied by the horizontal hydraulic jack. Axial and lateral loadings were controlled by two different loading systems.

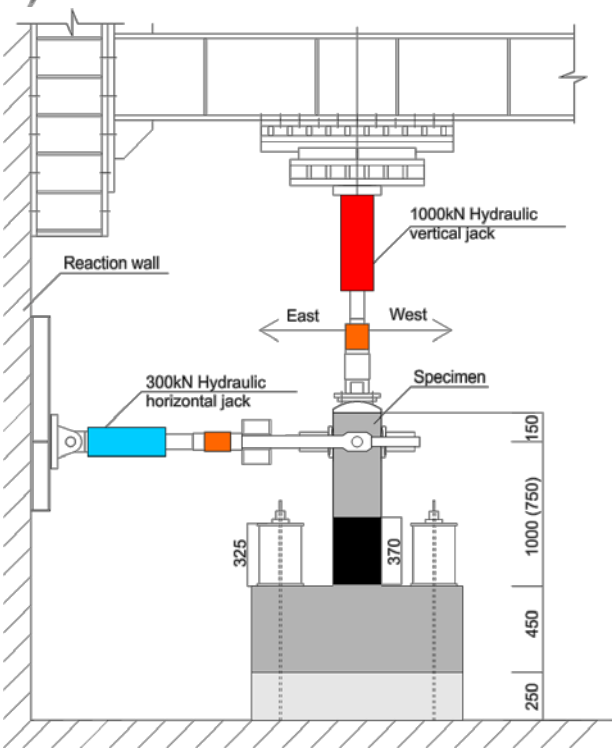


Fig. 3 Schematic view of test apparatus

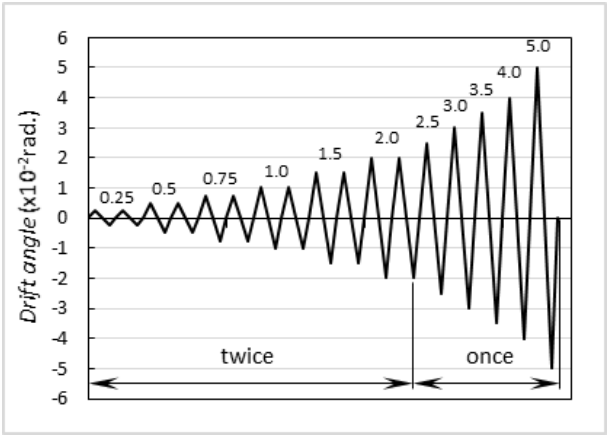


Fig. 4 Loading program

One displacement transducer (DT) was installed to measure the lateral displacement and four DTs were installed to measure the overall axial displacement and local axial displacement within the end 1.5D region of the specimens.

The lateral loading was controlled by drift ratio (R) of column, which is defined as the ratio of the lateral displacement at the loading point of lateral force (Δ) to the shear span (a) of each column when constant axial load attained the target level. Two complete cycles were applied at each level of lateral displacement till drift ratio reached 0.02 rad, and one cycle was applied at each level displacement after drift ratio becomes larger than 0.02rad. The loading program is illustrated in Fig. 4.

After completion of a predetermined loading program, we performed additional loadings to find out the maximum strength of the columns. For specimens with shear span ratios of 3 and 4, the final drift ratios reached 0.08 rad. and 0.09 rad, respectively. Both final drift ratios were the upper limit of the stroke of the horizontal jack. Example of the final loading state is shown in Fig. 5.


Fig. 5 Ultimate final state of specimen

# 3. Experimental results and discussions

## 3.1 Cracks and damages of specimens

Fig. 6 shows crack patterns of all specimens. The blue and red lines represent the loading in push (West) and pull (East) directions, respectively. Cracks and damages of the columns were observed after tests by removing the steel plates. Only few cracks and slight damage were observed though the specimens under high axial compression had experienced large drift up to 0.08 rad. In the specimens with shear span ratio of 3, flexural cracks were generated about 375 mm upper from column base, while in the specimens with shear span ratio of 4, flexural cracks were spread about 500 mm upper from column base. Distribution of flexural crack implies that the length of hinge region of concrete columns is associated with the shear span of columns.

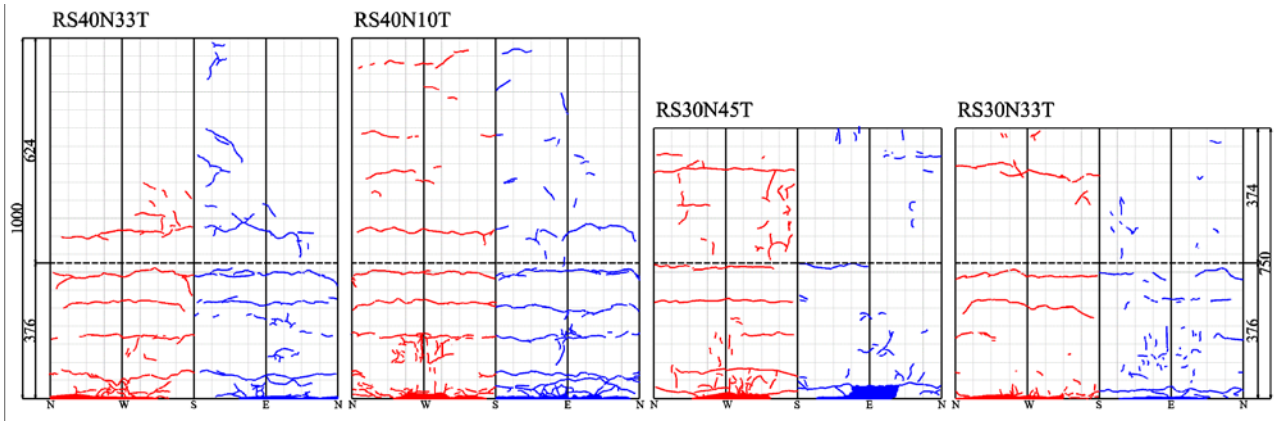


Fig. 6 Cracks and damages observed on specimens

## 3.2 Lateral force versus drift ratio relationships of specimens

The lateral load versus drift ratio hysteretic responses of all specimens are shown in Fig. 7. The solid circles superimposed in Fig. 7 represent the peak loading in the measured hysteretic curves, while the dotted lines in each graph expresses the so-called P-Δ mechanism lines.

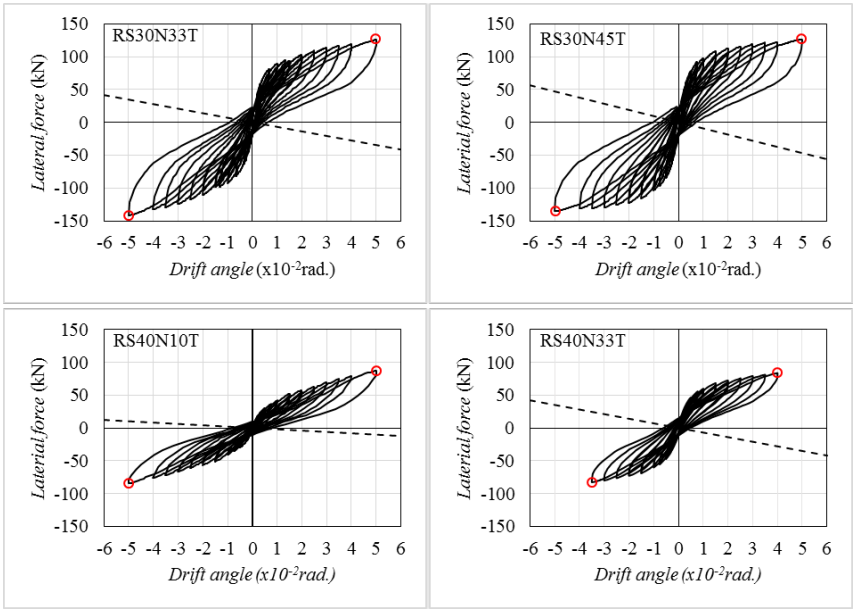


Fig. 7 Measured hysteretic lateral load versus drift ratio relationships

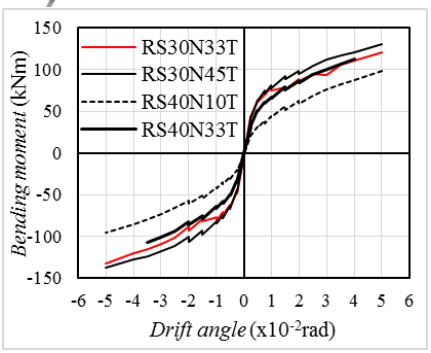


Fig. 8 Measured bending moment-drift ratio relatioships

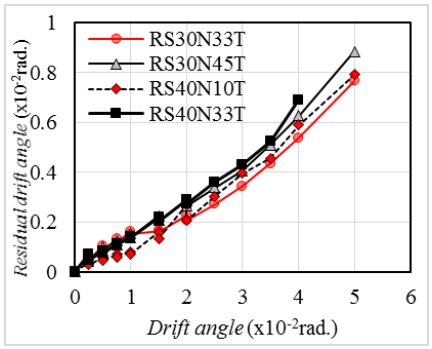


Fig. 9 Measured residual drift ratio

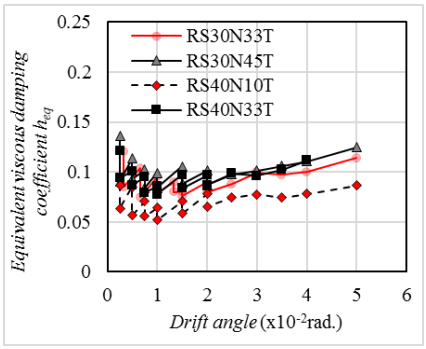


Fig. 10 Measured equivalent viscous damping coefficient

As can be seen from Fig. 7, the lateral resistance of columns with UHS rebars stably increased up to such a large drift level as 0.05 rad., without any deterioration in lateral load carrying capacity even when the columns were subjected to high axial compression loads with axial load ratio of 0.33 or 0.45.

To see the influence of shear span ratio on mechanical properties of drift-hardening columns, comparisons were conducted in terms of the moment at the end section versus drift ratio envelope curves in Fig. 8. From comparison of specimens RS30N33T and RS40N33T, only slight difference was observed between these two specimens, which implies that the influence of shear span ratio on the flexural property can be ignored.

Fig. 9 shows the experimental results of residual drift angle. In all specimens the residual drift angles were kept under a very low level until R = 0.05rad.

Fig. 10 shows the experimental results of the equivalent viscous damping coefficient (EVDC) of all columns. The higher the axial load ratio, the larger the equivalent viscous damping coefficient. It is interesting to note that the equivalent viscous coefficients were approximately constant until R reached 0.05rad, which implies that the columns behave in a non-linear elastic manner till large drift ratios.

## 3.3 Strains of longitudinal rebars

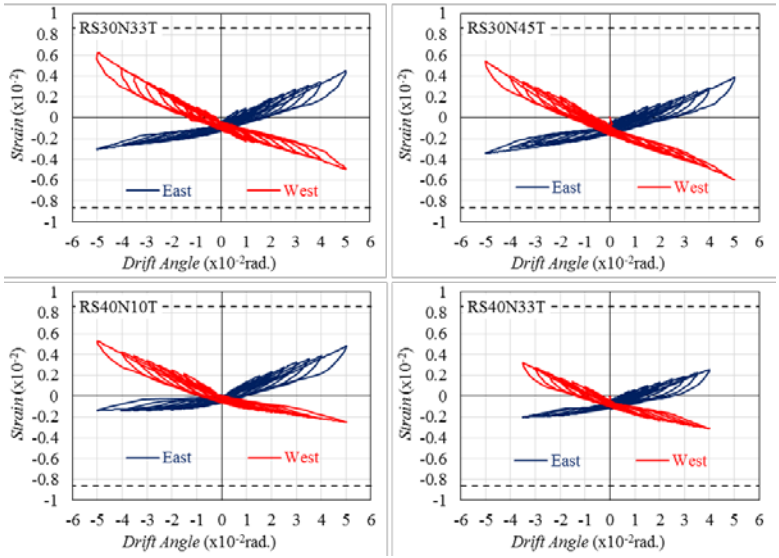


Fig. 11 Strains main reinforcement

Fig. 11 shows strains of longitudinal rebars reinforcement measured near at the section 25mm away from the column base for all specimens. The terms “East” and “West” in Fig. 11 represent the strains measured at the

initially tensile and compressive sides of column section, respectively, while the dashed horizontal lines represent the yield strain (0.84%) of UHS rebar. Along with the increasing of drift ratio, the steel strains exhibited stable increment, but did not reach its yield strain till the end of loading. The low bond strength delayed the yielding of UHS rebar and brought about the drift-hardening effect to concrete columns.

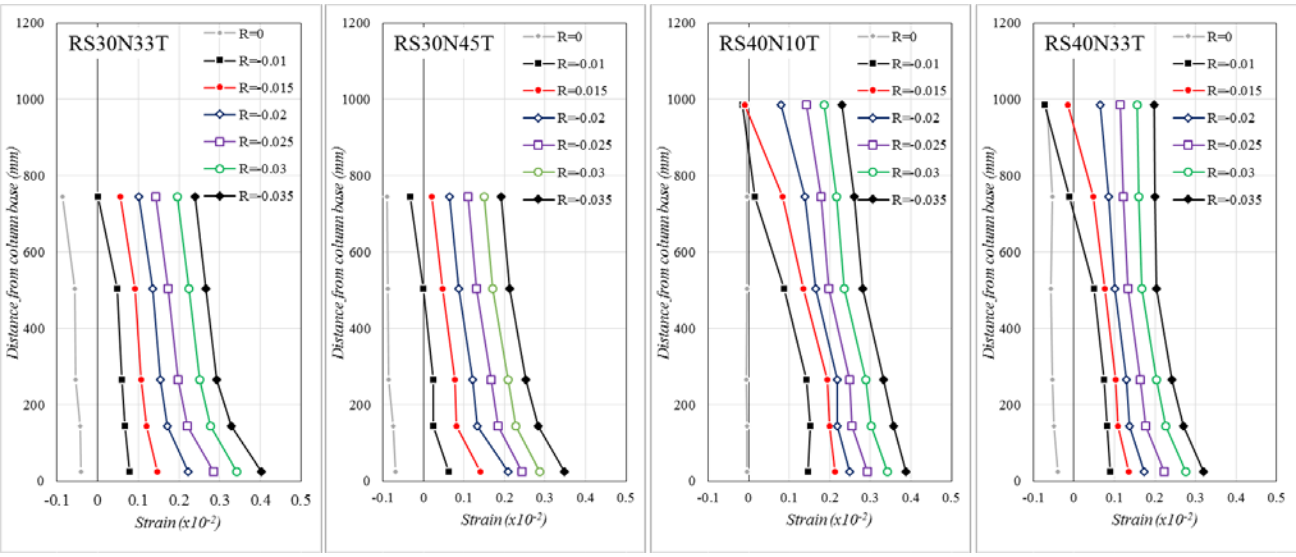


Fig. 12 Strains distribution of main reinforcement

Fig 12 shows the strain distribution of UHS rebars along the column height. The strains shown in Fig. 12 are those measured at several controlling drift ratios. As one can see that the strain gradient along the column height was very small and that the steel strains outside the end region exhibited approximately the same value as those within the end region. It is the wider distribution of steel strains that delays the yielding of UHS rebars and leads to high drift-hardening effect.

## 4. Analytical method for estimating cyclic performance of the suggested columns

As can be noticed from the previous section, the UHS SBPDN1275/1420 rebars didn't yield even when drift ratio reached 0.05 rad. and the slippage of rebars was unavoidable. Therefore, to reasonably evaluate the cyclic behavior of this type of structural components or members, a new analytical method that can take effect of slippage of longitudinal rebar into consideration is desirable.

### 4.1 Basic assumptions and analysis procedures

To simulate cyclic behavior of circular columns reinforced by UHS rebars and steel plates, the following basic assumption are made: 1) concrete does not resist tensile stress, 2) the concrete plane remains plane after bending, 3) the constitutive laws of the UHS rebars and the concrete are known [2-4] as shown in Fig. 13, 4) the bond-slip relationship of the UHS rebar follows the model developed by Funato et al [1] as shown in Fig. 14, 5) the lateral displacement of column concentrate in the plastic hinge region of 1.0D (D is the section diameter of member), 6) strain and stress of the UHS rebar are uniformly distributed within the plastic hinge region, 7) the bond strength of UHS rebar is taken as 3 N/mm$^2$ for the concrete with compressive strength of 40 N/mm$^2$ [1].

In the stress-strain relationship for the concrete confined by steel plates shown in Fig. 13, $\varepsilon_c$ and $f_c$ are the concrete strain and stress, respectively; $f_p$ and $\varepsilon_o$ are the compressive strength and corresponding strain for unconfined concrete, respectively; $f'_{cc}$ and $\varepsilon_o$ are the strength of confined concrete and corresponding strain, respectively; $f'_c$ is the strength of standard concrete cylinder with diameter of 100mm and height of 200mm; $E_c$ is the Young's modulus of concrete; $\rho_h$ is the volumetric ratio of circular hoops; $f_{yh}$ is the yield strength of hoops;

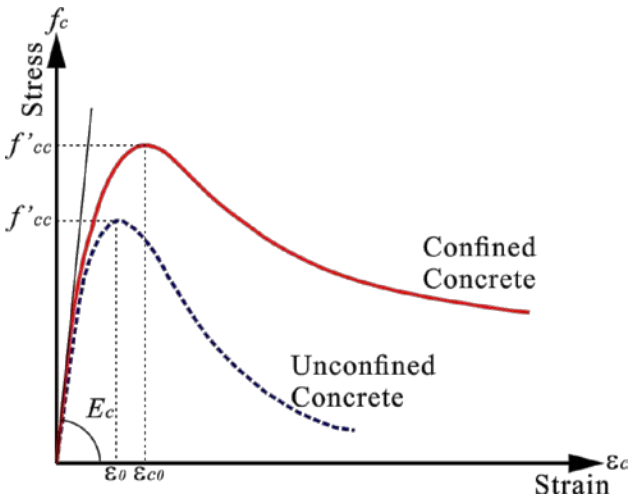


$$f_c = Kf_p' \frac{AX + (D-1)X^2}{1 + (A-2)X + DX^2}$$

$$f_p' = 0.85 f_c' \qquad X = \frac{\varepsilon_c}{\varepsilon_{c0}} \qquad A = \frac{E_c}{E_{sec}} = \frac{E_c \varepsilon_{c0}}{Kf_p}$$

$$D = 2.25 - 0.017 f_p' + \gamma \sqrt{\frac{(K-1)f_p'}{23}}$$

$$K = \frac{f_{cc}'}{f_p'} = \begin{cases} 1 + 2.05\left(1 - \dfrac{s}{2D_c}\right)^2 \dfrac{\rho_h f_{yh}}{f_p'} & for\ hoop \\ 1 + 4.1\left(\dfrac{2}{D'/t - 2}\right)\dfrac{f_{yt}}{f_p'} & for\ tube \end{cases}$$

Fig. 13 The stress-strain model of concrete [2-4]

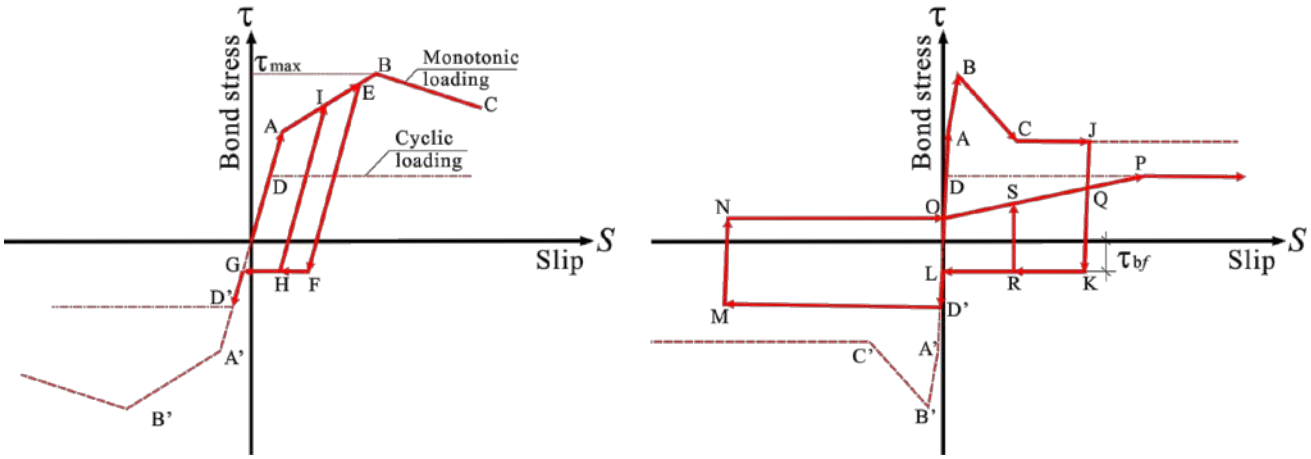


Fig. 14 The bond stress-slip relationship of UHS rebar in concrete [1]

$f_{yt}$ is the yield strength of steel plate; $K$ is the enhancement ratio of confined concrete; D and $t$ are the external diameter and thickness of steel plate, respectively; and $s$ is the spacing of circular hoops.

## 4.2 Comparison between measured and calculated results

Due to the limit of file size, only two examples of comparison are shown in Fig. 15, where illustrates the lateral load versus drift ratio curve, the residual drift corresponding to specific drift level, and the equivalent viscous damping coefficient for specimens RS30N33T and RS40N33T, each of which is representative of the specimens with shear span ratios of 3.0 and 4.0, respectively.

As one can see from Fig 15, the calculated results seem to underestimate the measured ones in all aspects. The difference between the calculated and measured lateral resistance becomes large along with drift ratio after R=0.01 rad. This discrepancy can be attrubited to two reasons; 1) ignorance of confinement effect of the core concrete by hoops (See Fig. 16) , 2) ignorance of confinement effect by steel plate on the slip resisting capacity of UHS rebar. The confinement effect of the core conrete by hoops can be taken into account by dividing the column section into core and cover portions, and assigning different strength enhancement ratio (K) to them as expressed in form of Eqs. (1) and (2). The effect by steel plate on the slip-resisting capacity can be considered by modifying the $\tau_{bf}$ that is defined in Fig. 14.

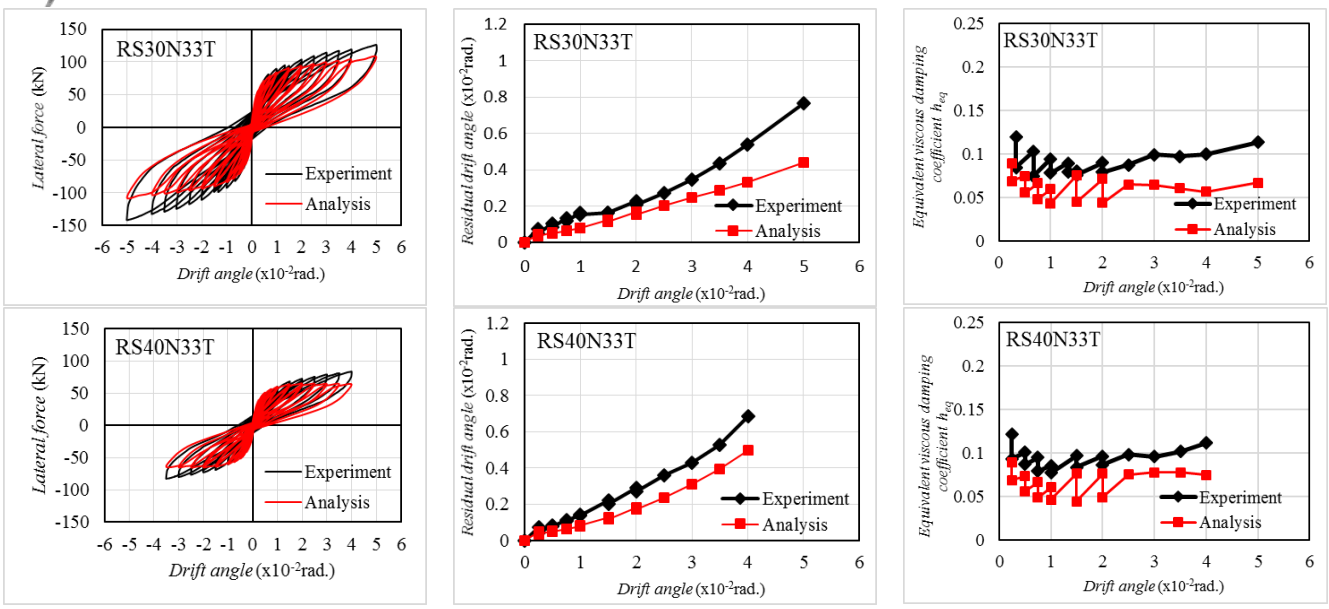


(a) Lateral load – drift ratio curves (b) Residual drift ratio (c) EVDC

Fig. 15 Comparisons between measured and theoretical results

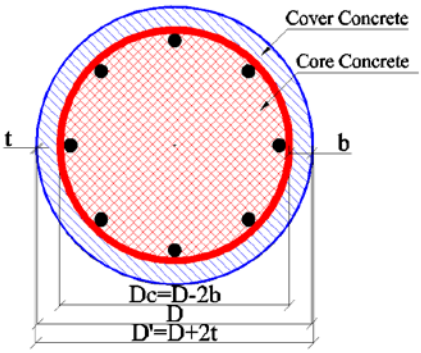


$$K_{cover} = 1 + 4.1\left(\frac{2}{D'/t - 2}\right)\frac{f_{yt}}{f_p'} \quad (1)$$

$$K_{core} = 1 + 4.1\left(\frac{2}{D'/t - 2}\right)\frac{f_{yt}}{f_p'} + 2.05\left(1 - \frac{s}{2D_c}\right)\frac{\rho_h f_{yh}}{f_p'} \quad (2)$$

Fig. 16 Definition of core and cover concrete

According to fib model [6], $\tau_{bf}$ for ordinary deformed rebar embedded in well-confined concrete can be taken as $0.4\tau_{max}$. In this paper, considering the low bond strength and the initial value $\tau_{bf}$ ($0.13\tau_{max}$) [1] of UHS rebar, $0.25\tau_{max}$ will be assumed for the UHS rebar embedded in steel plate-confined concrete.

The modified analytical results are compared with the measured ones in Fig. 17. One can see from Fig. 17 that properly considering the confinement effect by circular hoops on the core concrete strength and the confinement effect by steel plate on the slip-resisting capacity of UHS rebar can improve accuracy of the calculated results in aspects of hysteresis loop, residual drift and EVDC of the circular concrete columns reinforced with UHS rebars.

## 5. Conclusion

To develop a new type of high seismic performance concrete structures, four circular RC columns confined by thin steel plates and reinforced with UHS rebars were made and tested under reversed cyclic lateral force. Based on the experimental and analytical results described in this paper, the following conclusions cab be drawn:

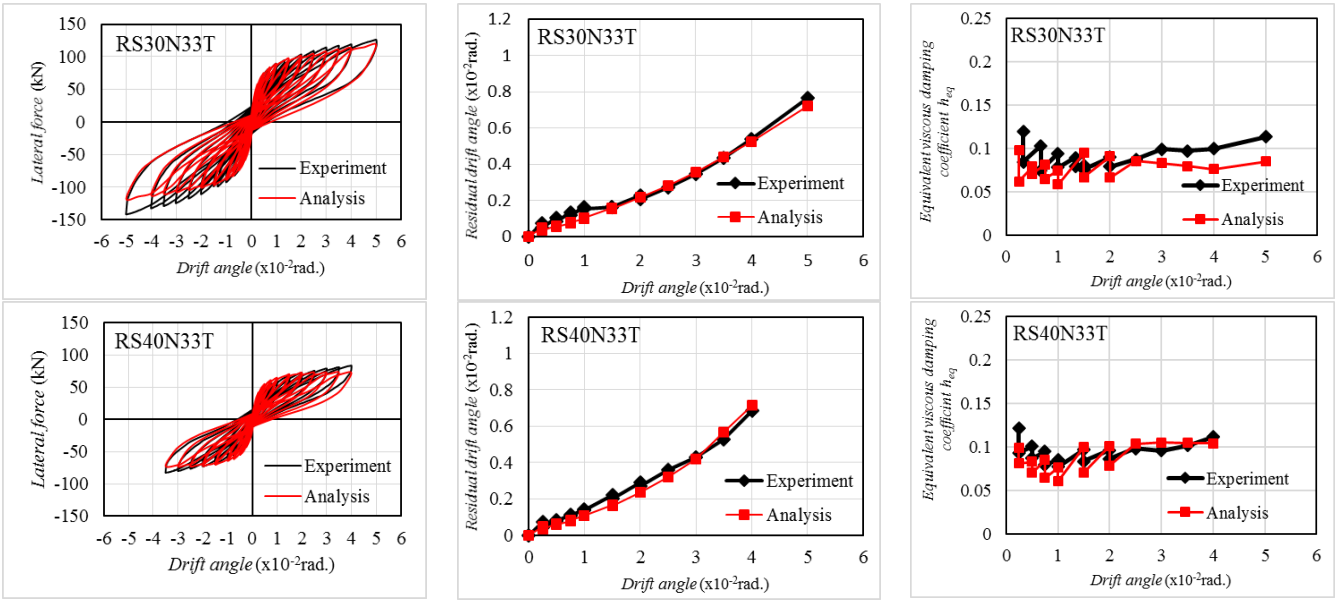


(a) Lateral load – drift ratio curves (b) Residual drift ratio (c) EVDC

Fig. 17 Comparisons between measured and modified analytical results

1) Combination of steel plate confinement and UHS rebars with low bond strength is very effective in making a drift-hardening concrete column. The circular RC columns confined by thin steel plates and reinforced with UHS rebars exhibited stable increment in lateral resistance along with drift ratio until 0.05 rad.

2) The residual drift ratios of all specimens were very small, and were about 15% of the experienced peak drift rations. The low bond strength of the used UHS rebars delayed the yielding of longitudinal steels and brought about the high drift-hardening effect to concrete columns.

3) The proposed analytical method can take effect of the slippage of UHS rebar and confinement effect by steel plate into consideration. The calculated results by the proposed method agreed very well with the test results in aspects of hysteresis loop, residual drift angle and equivalent viscous damping coefficient.

## Acknowledgment

The ultra-high strength rebars were provided by Neturen Co. Ltd. Their support is greatly appreciated.

## 6. References

[1] Funato Y., Sun Y., Takeuchi T., Cai G. (2012): Modeling and application of bond characteristic of high-strength reinforcing bar with spiral grooves, *Proceedings of the Japan Concrete Institute*, 34(2), 157-162, (in Japanese).

[2] Sun Y., Sakino K., Yoshioka T. (1996): Flexural behavior of high-strength RC columns confined by rectilinear reinforcement, *Journal of Structural and Construction Engineering*, Architectural Institute of Japan, No. 486, 95-106.

[3] Sun Y. et al. (2006), Modeling of complete stress-strain relationship for high-strength steels, *The First European Conference on Earthquake and Seismology*, Paper No. 760 (10 pages).

[4] Sun Y. et al. (2006), Analytical Study of Cyclic Response of Concrete Members Made of High-Strength Materials, *The Eighth U.S. National Conference on Earthquake Engineering*, Paper No. 1581 (10 pages).

[5] Sargsyan G., Tanaka Y., Takeuchi T., Sun Y. (2016): Seismic behavior and assessment of circular concrete columns reinforced by ultra-high strength rebars, *Proceedings of the Japan Concrete Institute*, (to be published).

[6] International Federation for Structural Concrete (2013): *The fib Model code for concrete structures 2010*, Wilhelm Ernst & Sohn, Berlin, Germany.